[CANCER RESEARCH 62, 2162–2168, April 1, 2002]

Persistence of Solitary Mammary Carcinoma Cells in a Secondary Site: A Possible Contributor to Dormancy[1]

George N. Naumov, Ian C. MacDonald, Pascal M. Weinmeister, Nancy Kerkvliet, Kishore V. Nadkarni, Sylvia M. Wilson, Vincent L. Morris, Alan C. Groom, and Ann F. Chambers[2]

Departments of Medical Biophysics [G. N. N., I. C. M., K. V. N., V. L. M., A. C. G., A. F. C.], Microbiology and Immunology [V. L. M.], and Oncology [V. L. M., A. F. C.], University of Western Ontario, London, Ontario, N6A 5C1 Canada, and London Regional Cancer Centre, London, Ontario, N6A 4L6 Canada [G. N. N., P. M. W., N. K., S. M. W., A. F. C.]

ABSTRACT

Tumors can recur years after treatment, and breast cancer is especially noted for long periods of dormancy. The status of the cancer during this period is poorly understood. As a model to study mechanisms of dormancy, we used murine D2.0R mammary carcinoma cells, which are poorly metastatic but form occasional metastases in liver and other organs after long latency. Highly metastatic D2A1 cells provided a positive, metastatic control. Our goals were to learn how the cell lines differ in survival kinetics in a secondary site and to seek evidence for the source of D2.0R dormancy. In spontaneous metastasis assays from mammary fat pad injections, we found evidence for dormancy because of a persistence of large numbers of solitary cells in the liver. To quantify the fate of cells after arrival in liver, experimental metastasis assays were used. To permit identification of cells that had not divided, cells were labeled before injection with fluorescent nanospheres, which were diluted to undetectable levels by cell division. Cancer cells were injected i.v. to target them to the liver and coinjected with reference microspheres to monitor cell survival. Dormancy was defined as retention of nanosphere fluorescence *in vivo*, as well as negative staining for the proliferation marker Ki67. A large proportion of D2.0R cells persisted as solitary dormant cells. No metastases formed, but viable cells could be recovered from the liver 11 weeks after injection. Large numbers of solitary, dormant, Ki67-negative D2A1 cells were also detected against a background of progressively growing metastases. Thus, this study identified a possible contributor to tumor dormancy: solitary, dormant cells that persist in tissue. If such cells are present in patients, they could contribute to tumor recurrence and would not be susceptible to current therapeutic strategies targeting proliferating cells.

INTRODUCTION

Metastasis is responsible for most breast cancer deaths, and it can occur many years after treatment of the primary tumor. Breast cancer commonly metastasizes to lung, bone, lymph nodes, liver, and brain (1, 2). Whereas the probability of recurrence can be estimated from various prognostic factors (3), limited understanding of the biology of the disease makes treatment decisions difficult and leads to years of uncertainty for patients.

Tumor dormancy has long been recognized clinically (4, 5). However, the status of the cancer between the time of primary treatment and metastatic recurrence remains poorly understood. Various factors have been identified as possible contributors to dormancy and subsequent recurrence, including tumor angiogenesis, cell proliferation and cell cycle arrest, immune regulation, and cancer cell interactions with the microenvironment (6–9). One contributor to dormancy is thought to be active but preangiogenic micrometastases in which proliferation and apoptosis are balanced (10, 11). These "dormant" micrometastases could be triggered to expand when host or cancer cell factors change to promote vascularization and progressive growth (12, 13). However, recent advances in quantification of early steps in metastasis have suggested another potential contributor to dormancy, namely the survival in tissue of solitary cancer cells that are neither proliferating nor undergoing apoptosis (14–16). If these quiescent cells remain viable in sufficiently large numbers, they could contribute to metastatic recurrence after a period of clinical dormancy.

Evidence for such cells was provided by Luzzi *et al.* (14), who found a large population of solitary cells against a background of rapidly growing liver metastases of B16F1 melanoma cells. Similar solitary cells were also observed in the liver for both metastatic and poorly metastatic mammary carcinoma cell lines (16). However, whether large numbers of such cells survive *in vivo* for extended periods of time is not known, and the kinetics of these cells have not been studied.

Here we used a murine model of breast cancer dormancy to study the survival kinetics of such dormant cells in liver. D2.0R cells are tumorigenic but poorly metastatic after injection either i.v. or into mammary fat pads (16, 17); these cells can form occasional metastases in lung or liver in some mice after long latency times (17). Thus, D2.0R cells provide a model for aspects of human breast cancer dormancy. In contrast, D2A1 cells are related but highly metastatic cells, which form metastases in lung, liver, and other organs of mice after either injection route (16, 17), and were used as a positive metastatic control.

Our goals in this study were to learn how the cell lines differ in their survival kinetics and to seek evidence for the source of dormancy for the D2.0R cells. We found that isolated cancer cells could be detected in mouse liver after implantation of both cell types to form primary mammary fat pad tumors. To quantify the survival and growth of such cells over time, we used experimental metastasis assays in which the cells were injected into the circulation to target them directly to the liver. We used a combination of IVVM[3] and detailed kinetic analyses, coupled with a fluorescent labeling strategy designed to assess whether cells had undergone cell division, to quantify the survival and growth of such cells at various times after mesenteric vein injection. This analytical approach permitted detection of a surprisingly large proportion of both cell types that persisted as solitary dormant cells, which retained nanosphere fluorescence and were negative for the proliferation marker Ki67. To assess the viability of these quiescent cells, D2.0R cells were recovered from the tissue and found to be viable as defined by the ability to both grow in cell culture and form tumors when reinjected in the mammary fat pad. Quantitative analysis of the fate of mammary carcinoma cells at a secondary site over time has thus revealed a potential source of dormancy for breast cancer and other cancers: solitary dormant cells that may remain viable for long periods of time.

Received 2/28/01; accepted 2/14/02.

The costs of publication of this article were defrayed in part by the payment of page charges. This article must therefore be hereby marked *advertisement* in accordance with 18 U.S.C. Section 1734 solely to indicate this fact.

[1] Supported by Canadian Institutes of Health Research Grant 42511 and an award from the Lloyd Carr-Harris Foundation. G. N. N. was supported by a Predoctoral Traineeship Award from the United States Army Breast Cancer Research Program (DOD DAMD17-00-1-0501).

[2] To whom requests for reprints should be addressed, at London Regional Cancer Centre, 790 Commissioners Road East, London, Ontario, N6A 4L6 Canada. Phone: (519) 685-8652; Fax: (519) 685-8646, E-mail: ann.chambers@Lrcc.on.ca.

[3] The abbreviations used are: IVVM, *in vivo* videomicroscopy; TUNEL, terminal deoxynucleotidyl transferase-mediated nick end labeling.

MATERIALS AND METHODS

Cell Culture and Fluorescent Labeling. D2A1/R and D2.0R/R murine mammary carcinoma cell lines [D2A1 and D2.0R cells (16–18) transfected with the pEGFP-C2 vector containing the *EGFP* (enhanced green fluorescent protein) gene and *neomycin* gene as a selectable G418 resistance marker] were maintained in tissue culture (37°C, 5% CO_2 humidified atmosphere) in DMEM (Canadian Life Technologies, Inc., Burlington, Ontario, Canada), supplemented with 10% FCS (Canadian Life Technologies, Inc.). The green fluorescent protein expression in these cells was not sufficiently strong to permit detection of cells *in vivo* based on green fluorescent protein fluorescence; however, the G418 resistance marker was stable and provided the means to select and characterize cells recovered from the liver 11 weeks after injection.

Cells for injection were fluorescence labeled (*green*) using fluoresbrite carboxylated polystyrene nanospheres of 48 nm in diameter (Polysciences, Warrington, PA), as described previously (14, 16). This procedure was used to provide a transient marker for the cells, aiding in detection of cells that had not undergone cell division. The nanospheres were spontaneously incorporated by the cells and retained in the cytoplasm. Labeled cells, from subconfluent monolayers, were harvested by trypsinization and resuspended in DMEM and 10% FCS to a final concentration of 2×10^6 cells/ml. Before injection, it was determined by fluorescence microscopy that >95% of the cells excluded ethidium bromide, indicating that membrane integrity was maintained (18, 19).

To quantify the initial fluorescence distribution in the nanosphere-labeled cells and the dilution of the fluorescence signal with cell division, D2.0R/R cells were grown under *in vitro* conditions to approximately 60% confluence and then fluorescence labeled (*green*) with a sterile nanosphere solution as described above. After a 2-h incubation, the cells were washed three times with PBS and trypsinized. Labeled cells were diluted and plated at limiting dilution in 96-well dishes (Nunc; Canadian Life Technologies, Inc.). Plates were then screened for wells containing a single cell. The same individual cells were documented and followed through one, two, and three or more cell divisions. Epifluorescence and transillumination images were obtained using a videocamera (Sony DXC-950) and stored for image analysis. Semiautomated analysis of the obtained digital images was performed using Optimas software (version 6.1; Optimas Co., Bothell, WA). For each image, the individual cell fluorescence intensity value was obtained after an appropriate background correction.

Initial fluorescence distribution in the nanosphere-labeled cells was also assessed by flow cytometry (Epics XL-MCL; Coulter, Miami, FL). For each sample (before and after nanosphere labeling), 10,000 cell counts were performed in triplicate.

Spontaneous Metastasis Assay. Female severe combined immunodeficient mice, 6–7 weeks of age (Charles River, St. Constant, Quebec, Canada), were cared for in accordance with the standards of the Canadian Council on Animal Care, under an approved protocol of the University of Western Ontario Council on Animal Care. Mice were anesthetized using a ketamine/xylazine mixture (1.6 mg ketamine and 0.08 mg xylazine/15 g body mass) administered by i.p. injection. A suspension of 3×10^5 D2A1/R, D2.0R/R, or D2.0R/R-REC (see below) cells in 0.2 ml of DMEM supplemented with 10% FCS was injected into an inguinal mammary fat pad, as described previously (17). Buprenorphine analgesic (Temgesic; 0.1 mg/kg body weight) was administered s.c. as mice awoke and 24 h after surgery.

Primary tumors of at least 9 mice/time point (3 times/week), for all three cell lines, were measured for size (mean diameter was calculated from the widest and right angle diameters). The primary tumors and livers obtained at the end point of the experiment were fixed in 10% neutral buffered formalin (pH 7.6) and examined for visible surface tumors and by histology.

Experimental Metastasis Assay. Female severe combined immunodeficient mice, 6–7 weeks of age, were anesthetized using a ketamine/xylazine mixture administered by i.p. injection. A suspension of 3×10^5 fluorescent nanosphere-labeled D2A1/R or D2.0R/R cells and 6×10^4 orange microspheres (see "Cell Accounting in Tissue") in 0.2 ml of DMEM supplemented with 10% FCS was injected into the superior mesenteric vein of each mouse to target cells to the liver as described previously (14, 16, 18). Buprenorphine analgesic (0.1 mg/kg body weight) was administered s.c. as mice awoke and 24 h after surgery.

Mice received injections of D2A1 or D2.0R/R cells (at least 3 mice/time point for both cell lines, with the exception of one mouse at day 77 that received injection of D2.0R/R cells) and were examined by IVVM immediately (up to 90 min) after injection or 3, 10, 14, 18, and 21 days later, as described previously (14, 20). The liver obtained from a mouse that received injection of D2.0R/R cells was examined at 11 weeks after injection and used for the cell recovery experiment described below. All livers obtained at the end point of the experiments were fixed in 10% neutral buffered formalin (pH 7.6) and examined for visible surface tumors. The fixed livers were sectioned (~50-μm thick) using a Vibratome Series 1000 sectioning system (Technical Products International, St. Louis, MO) as described previously (14). These thick sections were analyzed to determine the single cell and metastasis survival within the liver tissue at the eight time points after injection using the cell accounting technique (see below). Tissue adjacent to the thick section was embedded in paraffin for immunohistochemical analysis.

IVVM. The procedures for *in vivo* examinations of mouse liver using video microscopy have been described previously (14, 20). Briefly, in animals anesthetized with sodium pentobarbitol (60 mg/kg) i.p., a portion of a liver lobe was exposed, and the mouse was placed on a viewing platform on the stage of an epifluorescence inverted microscope. Oblique transillumination was provided by a fiber optic light source to enhance cell contrast, and epillumination (450–490 nm) was used to excite fluorescence-labeled cells and accounting microspheres. Real-time images obtained using a video camera (Sony CCD) were viewed on a video monitor and recorded on SVHS videotape. The animal's temperature was monitored and maintained at 37°C using a heat lamp. Anesthesia was maintained with supplemental administration of sodium pentobarbitol as required.

Cell Accounting in Tissues. To determine the proportions of injected cancer cells that extravasate and survive in the tissue or form metastases, it is necessary to express the number of cells observed in a tissue sample at various times, relative to the number of cells originally entering that volume. The cell accounting technique was developed for this purpose and has been described previously (14, 15, 20). Briefly, inert plastic microspheres of uniform size (10.2 ± 0.1 μm in diameter; orange fluorescence; Molecular Probes, Inc.) that remain trapped by size restriction within the microcirculation were injected together with the cancer cells in a known ratio (~5:1, cells:microspheres), providing a reference standard for monitoring cell survival at various later times. Formalin-fixed livers were cut into 50-μm thick sections, and at least five sections (400 μm apart) from the same lobe of each mouse liver were analyzed for solitary cell and metastasis survival. This procedure involves counting the number of microspheres in a particular volume to estimate the number of cells originally arrested and comparing this value with the number of cells observed in that same volume. Because the cells retain strong nanosphere fluorescence in the absence of cell division (detectable above the natural autofluorescence of the liver), dormant cells could be identified and quantified even at later time points. Dormancy was further defined as negative staining for Ki67 (see "Histology"). Cell accounting was also used to quantify survival of metastases based on the assumption that each metastasis originated from a single cell (21–23). Metastasis and microsphere counts were obtained from H&E-stained, 4-μm-thick sections.

Histology. Liver tissue adjacent to the 50-μm-thick sections described above was embedded in paraffin according to standard histological procedures. Representative sections were cut from primary mammary fat pad tumors and livers for animals that were given injections of D2A1/R, D2.0R/R, or D2.0R/R-REC-8 (see below) cell lines. For animals used in experimental metastasis assays, serial sections (4 μm) were cut from at least three different areas of a liver lobe, using at least 3 mice/time point. Sections were stained as follows: section 1 was stained with H&E; section 2 was stained using the TUNEL assay to assess apoptosis; and section 3 was stained with Ki67 (NCL-Ki67-MM1, monoclonal antibody; Dimension Laboratories, Mississauga, Ontario, Canada) to identify proliferating cells, as described previously (14).

Metastatic Burden and Survival. Sections stained with H&E were examined for evidence of disseminated solitary cancer cells. H&E-stained sections were also used to quantify tumor burden and metastasis survival, using 5 sections/mouse. To calculate tumor burden, the area occupied by tumor and total tissue area/section were measured. Tumor burden was then calculated as a percentage of organ volume, using stereological corrections (24). Section areas were quantified using Optimus software (Optimus Co.). Survival of metastatic foci was calculated as described above by counting the number of metastases and microspheres/section. To eliminate double and triple counting of the same metastases in serial tissue sections, unbiased stereological correc-

tion was used (24). The percentages of carcinoma cells staining positive for TUNEL or Ki67 were determined for (*a*) solitary cells within the tissue and (*b*) cells within tumors.

Cell Recovery from Liver Tissue. D2.0R/R cells were recovered from fresh liver tissue by dissociation into a single cell suspension and plated in G418-containing selective media, essentially as described previously (22, 25). This recovery procedure will underestimate the number of viable cells present (25) but is useful for documenting the presence of viable cells. Briefly, dissected livers were minced finely with crossed scalpels. The minced tissue was washed with calcium magnesium-free HBSS and enzymatically dissociated using collagenase-trypsin-DNase I [0.3% type IV collagenase (Roche Diagnostics, Montreal, Quebec, Canada), 0.2% trypsin (Bacto-trypsin; Difco Laboratories, Detroit, MI), and 50 μg/ml DNase I (Sigma Chemical Co.)] prepared in calcium magnesium-free HBSS solution. Tissue was incubated for 1 h at 37°C with periodic vortexing. Dissociated tissue was plated and maintained in DMEM and 10% FCS plus 1.5 μM G418 and incubated for 3–4 weeks under normal tissue culture conditions. At this predetermined concentration of G418, liver cells die rapidly, whereas the D2.0R/R cells grow to form G418-resistant colonies in the plates. Fifteen recovered clones, designated D2.0R/R-REC-1 to D2.0R/R-REC-15, were obtained. A representative clone, D2.0R/R-REC-8, was reinjected in the mammary fat pad, as described above (see "Spontaneous Metastasis Assay").

Statistical Analysis. Data are expressed as the mean ± SE. Statistical analyses were performed using Sigma Stat version 2.03 for Windows (Access Softek Inc., San Rafael, CA). To assess the relationship between specific factors, the appropriate Student's *t* test or Mann-Whitney test was performed. A level of $P < 0.05$ was regarded as statistically significant.

RESULTS

Growth of Mammary Fat Pad Tumors and Evidence for Metastatic Dormancy in Liver. Ten days after injection, all mice that received injections with D2A1 cells had visible tumors at the primary site ($n = 9$ mice; mean diameter, 8.8 ± 1.0 mm). Similar-sized tumors were found 25 days after injection of mice with D2.0R/R cells ($n = 10$ mice; mean diameter, 9.6 ± 1.0 mm). Upon histological examination, solitary cells were found in livers of mice bearing either D2A1/R or D2.0R/R primary tumors (Fig. 1*B*). These solitary cells were consistent morphologically with cells from the primary tumors (Fig. 1*A*). Positive identification and quantification were not possible because the cell lines proved to be negative for a variety of tumor markers tested (*e.g.*, cytokeratin AE1/AE3 [DAKO] negative, data not shown). Thus, to study the kinetics of solitary cell survival, experimental metastasis assays were used.

Characterization of Dilution of Nanosphere Fluorescence with Cell Division. To use nanosphere labeling of the cells as a marker for *in vivo* detection of dormant cells, we carried out the following control experiments *in vitro*: nanosphere-labeled D2.0R/R cells were cloned as single cells, and their fluorescence distribution was quantified before cell division ($n = 63$) and after one ($n = 25$), two ($n = 54$), or three or more ($n = 53$) cell divisions. Immediately after incubation with fluorescent nanospheres, the cells were found to be highly fluorescent as assessed microscopically (Fig. 2*a*). We quantified the

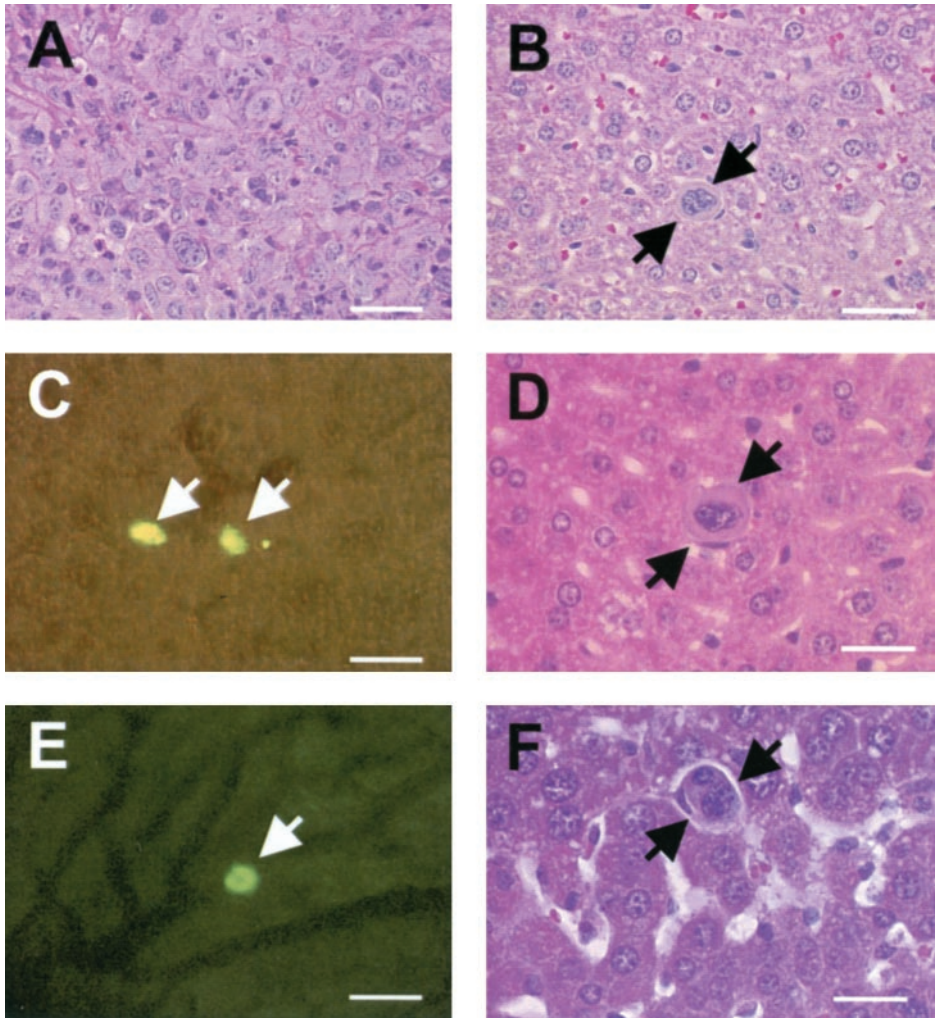

Fig. 1. Solitary dormant D2.0R/R and D2A1/R cells as detected *in vivo* and by histology. *A*, view from a H&E-stained section of a primary tumor in the mammary fat pad of a mouse injected with D2.0R/R cells (*bar*, 20 μm). *B*, an example of a solitary D2.0R/R cell (*arrows*) detected in the liver 25 days after injection in the mammary fat pad as part of a spontaneous metastasis assay. Such solitary cells, as detected in H&E-stained sections, were consistent morphologically with cells from the primary tumor (see *A*). Similar solitary cells were also found in the livers of mice injected in the mammary fat pad with D2A1 cells (data not shown; *bar*, 20 μm). *C*, fluorescence-labeled solitary D2.0R/R cells (*arrows*) were detected in liver tissue 11 weeks after injection to target the liver (*bar*, 20 μm). The image was obtained from a 50-μm-thick section. *D*, similar solitary D2.0R/R cell (*arrows*) 11 weeks after injection in H&E-stained liver section (*bar*, 15 μm). *E*, a fluorescence-labeled solitary D2A1/R cell (*arrows*) as detected by IVVM 21 days after injection (*bar*, 20 μm). The cell shown was confirmed to be extravascular by focusing through the tissue at high magnification (see the text). *F*, similar D2A1 solitary cell (*arrows*); H&E-stained section; 21 days (*bar*, 15 μm).

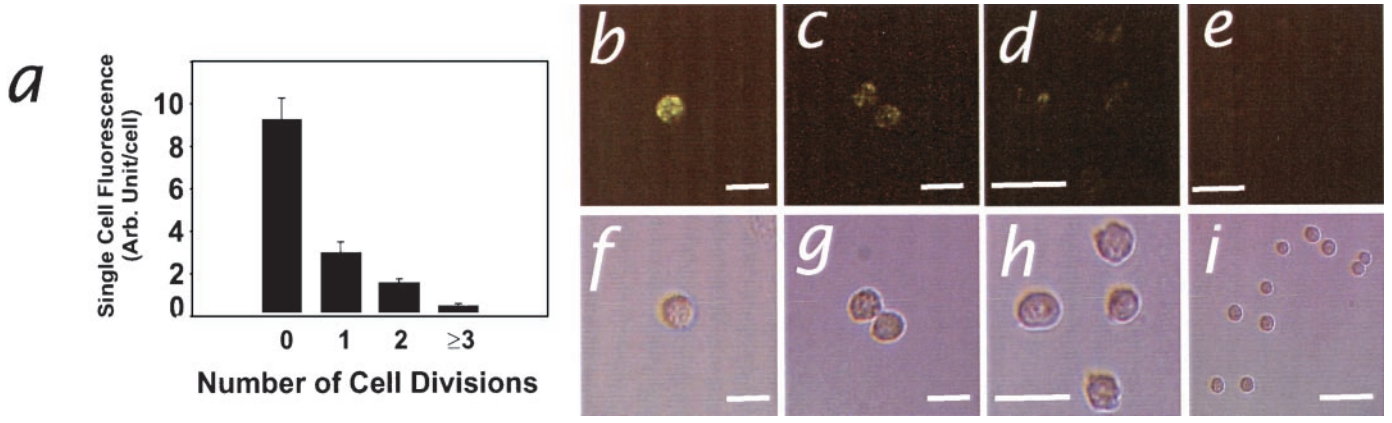

Fig. 2. Loss of fluorescence of single nanosphere-labeled D2.0R/R cells with consecutive cell divisions *in vitro*. *a*, the *bars* represent the mean fluorescence of individual cells that have not divided ($n = 63$) or have divided once ($n = 25$), twice ($n = 54$), or at least three times ($n = 53$) after initial nanosphere labeling. The loss of fluorescence in cells that had divided at least once was significant when compared with labeled cells that had not divided ($P < 0.001$, values at no cell division *versus* values for one, two, or at least three cell divisions). *Error bars*, SE. *b*−*i*, images of representative nanosphere-labeled D2.0R/R cells after consecutive divisions *in vitro*; *b*−*e*, epifluorescence images represent the mean fluorescence values graphed on *a*. Corresponding transillumination images of the cells in *b*−*e* are shown in *f*−*i*. Cells shown in *e* and *i* originated from the single cell shown in *b* and *f*. *Bar* = 20 μm in *b*, *c*, *d*, *f*, *g*, and *h*; *bar* = 40 μm in *e* and *i*.

heterogeneity of the initial fluorescence. Ninety percent of the nanosphere-labeled cells were within a 2.8-fold range of fluorescence intensity. This finding was confirmed by flow cytometry ($n = 10{,}000$ cells), where 90% of the cells were found to be within a 2.9-fold range of fluorescence intensity. Thus, although a small proportion of cells was outside this range, the majority of cells were within a tight distribution of fluorescence intensity.

The fluorescence of individual cells was diluted by successive cell divisions. This fluorescence was quantified (Fig. 2*a*), and representative images are shown in Fig. 2, *b*−*i*. In particular, a marked reduction in mean cellular fluorescence was found after a single cell division *in vitro*. Thus, the majority of labeled cells would not be detectable *in vivo* after a single division, above the background autofluorescence (Fig. 1, *C* and *E*) of the liver tissue. However, a small proportion of the cells might still be detectable *in vivo* after one or even two divisions.

Dormancy and Persistence of Large Numbers of Undivided but Viable D2.0R/R Cells after i.v. Injection to Liver. Cells were injected via the mesenteric vein to target them to the mouse liver. To identify solitary cancer cells that had not divided, the cells were labeled before injection with fluorescent 48-nm polystyrene nanospheres (14, 15).

No macroscopic metastases or micrometastases were formed in the D2.0R/R-injected mice at 3 or 11 weeks after injection, as detected by surface nodules or by histology. However, large numbers of solitary, brightly fluorescent D2.0R/R cells were detected in the liver at all time points, even 11 weeks after injection, in 50-μm tissue sections (Fig. 1*C*) and by IVVM (data not shown). These cells were morphologically consistent with malignant cells by standard histology (Fig. 1*D*). To determine if the apparently dormant D2.0R/R cells were viable, liver tissue was dissociated and plated *in vitro* in G418-containing selective medium 11 weeks after cell injection; these carcinoma cells carry the G418 resistance gene, permitting this selection. Viable, G418-resistant colonies grew out. Thus, some of the apparently dormant cells detected in the liver 11 weeks after injection retained the ability to grow under *in vitro* culture conditions. The recovered cells demonstrated *in vitro* morphology and growth kinetics identical to those of the parental D2.0R/R cells (data not shown). In addition, when reinjected in the mammary fat pad, recovered D2.0R/R cells (D2.0R/R-REC-8) successfully formed primary tumors in 10 of 10 mice, which were comparable in size after 35 days to those of the parental cell line (mean diameter, 9.6 ± 1.2 mm). This finding indicates that, despite their apparent dormancy at a secondary site, the recovered cells retained their tumorigenic phenotype.

Quantification of the Survival of Dormant D2.0R/R Cells in Liver Tissue. To quantify the kinetics of cell survival at successive steps in the metastatic process, we used an accounting technique using reference microspheres coinjected with the cells (14, 15). This technique allows us to express the number of cancer cells observed in a sampled volume of liver tissue at various times after injection, relative to the number of cells that originally entered that tissue volume. IVVM confirmed that immediately after injection, cancer cells and accounting microspheres were arrested by size restriction within periportal sinusoids, with immediate cessation of blood flow in these particular sinusoids. By 3 days, all observed cancer cells (of both cell types) had extravasated, whereas the reference microspheres remained within the sinusoids. The distinction between intravascular and extravasated cells was made possible by using IVVM at high magnification. Under these conditions, the depth of focus is less than the thickness of the cells or sinusoids. Thus, by focusing up and down through the tissue, it was possible to establish that these cells were extravascular.

D2.0R/R cells showed an initial loss of ~14% of injected cells shortly after injection (Fig. 3*a*). Thereafter, from 90 min to 21 days after injection, there was no significant loss of cells, and ~80% of the D2.0R/R cells remained as undivided cells. Even after 11 weeks, ~50% of the D2.0R/R cells that had been injected remained as solitary, brightly fluorescent cells. These cells were identified to be dormant by their retention of fluorescent nanospheres, detectable both by IVVM and in 50-μm-thick sections. Furthermore, such brightly fluorescent cells demonstrated consistently low levels of both apoptosis and proliferation, as assessed in histological sections by TUNEL (Fig. 3*b*) and Ki67 (Fig. 3*c*) staining, respectively. No Ki67-positive D2.0R/R cells were detected at days 21 or 77 (Fig. 3*c*). Thus, the brightly fluorescent cells detected showed histological evidence of dormancy.

Kinetics of Survival and Metastatic Growth of a Subset of D2A1 Cells. There was an initial loss (~11%) of the injected D2A1 cells within the vasculature shortly after injection (Fig. 4*a*), and by day 3, all remaining cells (~70% of injected cells) had extravasated. By day 10, ~64% of the injected cells still remained as undivided solitary cells (Fig. 4*a*); however, a small subpopulation of the injected cells (0.623%) had begun to form metastases (Fig. 5*a*), which occupied ~6% of the liver volume at this time (Fig. 5*d*). Not all of these

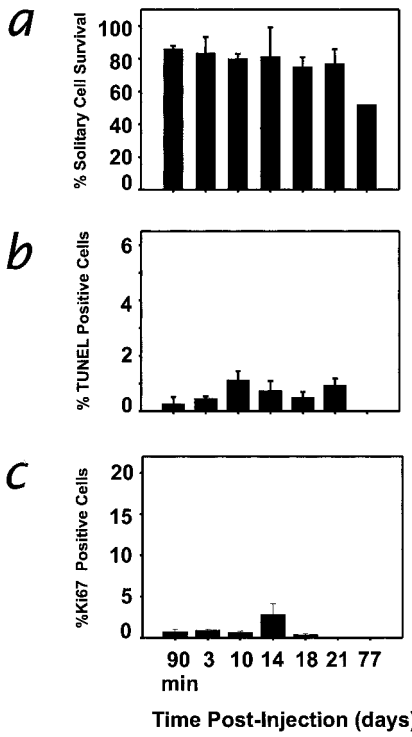

Fig. 3. Long-term survival of poorly metastatic (D2.0R/R) solitary cells in mouse liver. *a*, *in vivo* survival was assessed in 50-μm tissue sections by cell accounting. The initial cell loss during the first 90 min was significant ($P < 0.01$, values at 90 min *versus* 100%). High solitary cell survival was found for the poorly metastatic D2.0R/R cells even 11 weeks after injection. The *bars* represent mean survival of solitary cells as a percentage of cells initially injected. These solitary cells had consistently low levels of apoptosis (*b*) and proliferation (*c*) that did not differ from background levels observed in normal liver tissue at all time points. Apoptosis and proliferation levels in solitary D2.0R/R cells were quantified from TUNEL and Ki67-stained thin sections, respectively. *Error bars*, SE.

early metastases continued to grow, however, and their numbers decreased by a factor of 100 (0.623% of injected cells, day 10 *versus* 0.006% of injected cells, day 14) between days 10 and 14 (Fig. 5*a*), although total metastatic burden increased dramatically over this time (Fig. 5*d*). (This decrease in numbers of metastases could not be attributed to fusion of metastases, based on sizes and spacing of metastases up to this time point.) Coincident with this loss of early metastases was a second phase of loss of solitary cells between days 10 and 14 (Fig. 4*a*). In contrast to the dramatic loss of metastases during this interval (Fig. 5*a*), the number of solitary D2A1 cells (as reflected by the percentage of injected cells remaining as solitary cells) fell by only a factor of 3 (64%, day 10 *versus* 19%, day 14; Fig. 4*a*). These results indicate that the rate of loss of early metastases was almost 2 orders of magnitude greater than that for solitary cells.

By day 21, the tumor burden had increased to 73% of the liver volume (Fig. 5*d*), with an average of 50 macroscopic metastases/mouse as calculated from 50-μm-thick sections of the liver. (These counts were in good agreement with counts of surface tumors at day 21, which yielded an average of 32 macroscopic metastases/mouse.) This large tumor burden (Fig. 5*a*) was because of the growth of only a small subpopulation (0.006% at day 18) of the injected D2A1 cells, corresponding to an estimate of 30 metastases. This estimate is comparable with the average numbers of metastases detected at day 21, assuming metastases were essentially clonal.

Against this background of progressively increasing tumor burden because of the growth of a small subset of D2A1 cells, we thus detected the persistence of surprisingly large numbers of fluorescent cells at day 21 (~22% of the injected cells; Fig. 4*a*). When livers were examined using IVVM (Fig. 1*E*) or by standard histology (Fig. 1*F*) in regions distant from the growing metastases, the dormant cells were similar in appearance to those observed for the D2.0R/R cells (*cf.* Fig. 1, *C* and *D*).

Contribution of Apoptosis to Metastatic Inefficiency of D2A1 Cells. To examine possible mechanisms for the loss of D2A1 solitary cells and early metastases between 10 and 14 days, as well as to assess the dormancy of solitary cells observed at later times, we quantified apoptosis and proliferation by TUNEL and Ki67 staining in both solitary cells and the metastases. At most time points, apoptosis levels in solitary cells were low (<1%; Fig. 4*b*). However, a 4-fold increase in apoptotic solitary cells was found at day 14, and this peak of apoptosis occurred at the time of greatest single cell loss (*cf.* Fig. 4*a*). A similar peak of apoptosis was detected within the early metastases at day 14 (Fig. 5*b*) at the time of greatest loss of metastases (*cf.* Fig. 5*a*).

A high proportion of D2A1 cells populating metastases were Ki67-positive at all time points (Fig. 5*c*), consistent with active proliferation. In contrast, the majority of solitary D2A1 cells present were dormant, as defined by low levels of proliferation (Fig. 4*c*) and apoptosis (Fig. 4*b*). [Interestingly, whereas >85% of solitary D2A1 cells were negative for Ki67 at all time points (Fig. 4*c*), an even larger proportion (>95%) of solitary D2.0R/R cells were Ki67 negative (Fig. 3*c*).] Thus, cells within metastases and solitary dormant cells appear to be differentially regulated. Furthermore, the finding of persistence of dormant cells was observed for both the metastatic cell line and the poorly metastatic cell line.

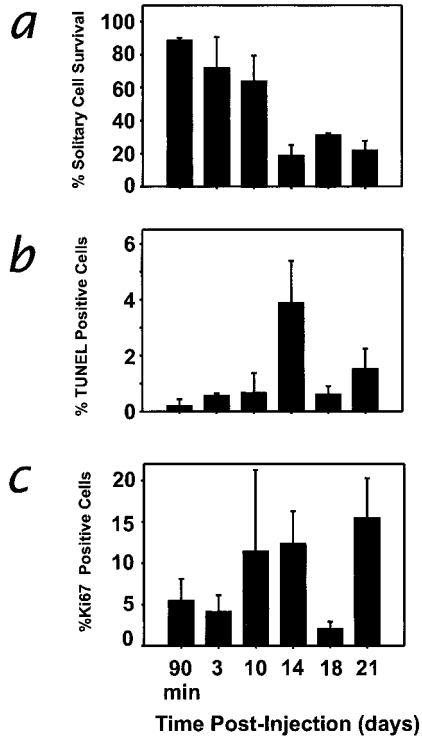

Fig. 4. Survival and loss of highly metastatic (D2A1/R) solitary cells in mouse liver. *a*, *in vivo* survival was assessed in thick tissue sections by cell accounting. The initial cell loss during the first 90 min was significant ($P < 0.01$, values at 90 min *versus* 100%). Subsequent loss for the D2A1/R cells over the next 10 days was not significant ($P = 0.5$, values at 90 min *versus* 10 days). By day 14, survival for solitary D2A1/R cells was significantly lower than that at the earlier three time points ($P < 0.01$), but approximately one-fourth of the cells originally injected still remained. Similar survival levels were found at day 21. The *bars* represent the mean survival of solitary cells as a percentage of cells initially injected. *b*, apoptosis levels in solitary D2A1/R cells as quantified from TUNEL-stained sections. A significant increase in the proportion of D2A1/R cells undergoing apoptosis was observed at day 14 ($P \leq 0.015$, values at 14 days *versus* all other time points). *c*, proliferation levels in solitary D2A1/R cells as quantified by Ki67 staining; none of the values at days 3–21 differ significantly from the value at 90 min ($P > 0.10$). *Error bars*, SE.

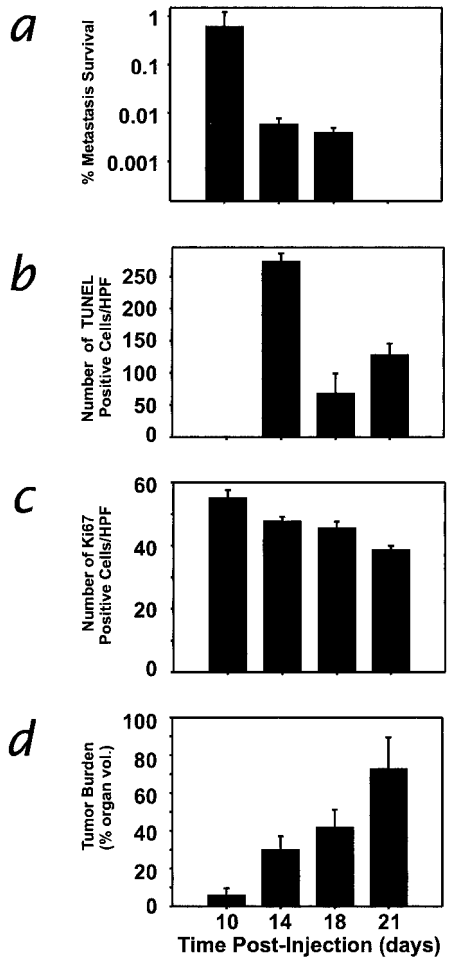

Fig. 5. Growth of D2A1/R metastases. *a*, the survival of metastases was calculated using the cell accounting procedure, assuming clonal origin (*i.e.*, each metastasis represents a single injected cell). A dramatic and significant loss of early D2A1/R metastases occurred between days 10 and 14 (survival corresponding to 0.623% and 0.006% of injected cells, respectively; $P < 0.01$). No metastasis survival data were available at day 21 because of fusion of metastases by this point. D2A1/R metastasis-bearing mice were killed at day 21 because of tumor burden. *b*, apoptosis within D2A1/R metastases, quantified as the number of TUNEL-positive cells within metastases/high power field. No apoptosis was detected within the early metastases observed at day 10. However, a significant peak of apoptosis was found at day 14 ($P < 0.01$, values at 14 days *versus* all other time points) compared with days 18 and 21. *c*, proliferation within metastases, quantified as the number of Ki67-positive cells within metastases/high power field. *d*, tumor burden was calculated as a percentage of the available liver volume occupied by metastases at days 10–21. *Error bars*, SE.

DISCUSSION

Tumor dormancy and subsequent metastatic recurrence are significant clinical problems responsible for much uncertainty in the treatment of cancer and, ultimately, for many cancer deaths (26–28). Initially, dormancy was considered to be because of a slow but steady growth of tumor cells seeded to distant organs before or during primary tumor removal (29). Such growth would eventually produce metastases of clinically detectable size. Contrary to the continuous tumor growth hypothesis, clinical considerations coupled with mathematical modeling suggested instead that metastases might have phases of both active and arrested growth (26, 27, 30–33). Despite the early clinical observations and mathematical modeling, little is known about the status of dormant tumor cells. Folkman's laboratory has documented the existence of preangiogenic metastases, which are metabolically active but functionally dormant because of a balance between apoptosis and proliferation (10, 11). Progressive growth in such tumors was restricted because of failure of the micrometastases to become vascularized. Here, we provide quantitative evidence for another possible source of tumor dormancy: solitary dormant but viable cells that are neither dividing nor undergoing apoptosis.

We found that a large percentage of mammary carcinoma cells, distributed to mouse liver via the circulation, can remain in the tissue for extended periods of time as solitary dormant cells. This phenomenon was detected for cell populations of both high and low metastatic ability. In the case of the highly metastatic cell line, metastases that gave rise to a large tumor burden were formed from a very small subset of cells (~0.006%), with the majority of injected cells dying (~80% cell loss by day 21) in association with peaks of apoptosis and (data not shown) leukocyte infiltration. However, a substantial fraction (~20%) of the injected cells persisted as dormant cells. For the poorly metastatic cell line, there was even less total cell loss, with 80% of injected cells remaining at day 21 and 50% of injected cells still present 11 weeks after injection. These solitary cells were dormant, as defined by both retention of nanosphere fluorescence and Ki67 negativity. At least some of these cells were shown to be viable, as defined by the ability to grow both in cell culture and *in vivo*. Such dormant cells would not have been detected by standard metastasis assays, in which only the end point of the process is assessed. Furthermore, routine histology could not be used to reliably detect and quantify solitary cancer cells. The detailed kinetic analyses of this study, afforded by a combination of recent advances in IVVM and quantitative cell accounting, permitted detection and quantification of a previously unappreciated population of dormant cells that remain during the metastatic process.

This study identified a number of features shared by the metastatic and poorly metastatic cell lines and several unique features that may contribute to their different metastatic end points. Both cell lines underwent a small but significant initial loss of cells from the liver immediately after injection, perhaps because of the cells' transit through the organ or rapid cell killing not detected by the apoptosis assay. [A recent study using rat embryo fibroblast cell lines has reported early solitary cell loss by apoptosis after hematogenous dissemination of the cells to the lung (34)]. Both cell lines subsequently persisted in large numbers in the tissue, until the point when a small subset of the metastatic cell line initiated cell division. Associated with this commencement of growth was a wave of apoptotic cell death and the loss of significant numbers of cells. However, for the metastatic cell line, large numbers of dormant solitary cells were detected above the background of progressively growing metastases. In the case of the poorly metastatic cell line, solitary cells persisted in large numbers and in a dormant state, and a subset of these cells could be recovered and grown under *in vitro* culture conditions 11 weeks after injection. These cells also retained the ability to form primary tumors after mammary fat pad injection. Thus, these cells may be a source of the tumor dormancy and occasional late metastasis formed by this cell line (17).

Two recent studies using metastasis-suppressed prostate and melanoma cell lines have obtained results that are consistent with the picture of dormancy that we present here. In both studies, the metastasis-suppressed cells were found to be able to arrest in the lungs, where they persisted but failed to grow (35, 36). In addition, reduction in surface urokinase plasminogen activator receptor expression in human carcinoma cells has been shown to impair their *in vivo* proliferation (in chick embryos), resulting in a protracted state of dormancy (9). Thus, dormancy and persistence of appreciable numbers of solitary cells in secondary sites may be a phenomenon that occurs in other cancer cell lines and various organs.

If our experimental observations reflect the clinical situation for breast and other cancers, the following question arises: are dormant cells more likely or less likely to persist in secondary sites for more

aggressive *versus* less aggressive primary tumors? For the cell lines we used, we found considerably more dormant cells in the nonmetastatic cell line. We found a wave of apoptosis in association with the initiation of cell division in a subset of cells of the metastatic cell line. This finding suggests that (*a*) cells may remain in a more protected state before initiation of cell division, and (*b*) cell division, even among a small subset of cells, may put other tumor cells in the organ at risk and increase the probability of their destruction.

The treatment of such dormant solitary cells in clinical situations could be problematic. Although "active" but preangiogenic metastases might be vulnerable to cytotoxic chemotherapeutic agents that target dividing cancer cells, solitary dormant cells should not be affected by this approach. For patients whose cancer is successfully treated, it is possible that dormant cells may remain, which might be unaffected by chemotherapy and retain the potential to begin growth at a later date. Furthermore, for patients treated successfully with new antiangiogenic therapies, a population of dormant cells unaffected by treatment may persist and regrow at a later time.

ACKNOWLEDGMENTS

We thank Leanne Reid and Karen Morley for assistance in the measurement of the mammary fat pad tumors, Dr. Alan Tuck (Pathology Department, London Health Sciences Center) for assistance in the analysis of tissue sections, and Michael Keeney (London Health Sciences Center) for assistance with flow cytometry. We also thank Drs. Patricia S. Steeg and Danny R. Welch for reading the manuscript and for helpful suggestions.

REFERENCES

1. Cifuentes, N., and Pickren, J. W. Metastases from carcinoma of mammary gland: an autopsy study. J. Surg. Oncol., *11:* 193–205, 1979.
2. Lee, Y. T. Breast carcinoma: pattern of metastasis at autopsy. J. Surg. Oncol., *23:* 175–180, 1983.
3. Fitzgibbons, P. L., Page, D. L., Weaver, D., Thor, A. D., Allred, D. C., Clark, G. M., Ruby, S. G., O'Malley, F., Simpson, J. F., Connolly, J. L., Hayes, D. F., Edge, S. B., Lichter, A., and Schnitt, S. J. Prognostic factors in breast cancer. College of American Pathologists consensus statement 1999. Arch. Pathol. Lab. Med., *124:* 966–978, 2000.
4. Demicheli, R., Abbattista, A., Miceli, R., Valagussa, P., and Bonadonna, G. Time distribution of the recurrence risk for breast cancer patients undergoing mastectomy: further support about the concept of tumor dormancy. Breast Cancer Res. Treat., *41:* 177–185, 1996.
5. Crowley, N. J., and Seigler, H. F. Relationship between disease-free interval and survival in patients with recurrent melanoma. Arch. Surg., *127:* 1303–1308, 1992.
6. Gimbrone, M. A., Jr., Leapman, S. B., Cotran, R. S., and Folkman, J. Tumor dormancy *in vivo* by prevention of neovascularization. J. Exp. Med., *136:* 261–276, 1972.
7. Michelson, S., and Leith, J. T. Dormancy, regression, and recurrence: towards a unifying theory of growth control. J. Theor. Biol., *169:* 327–338, 1994.
8. Stewart, T. H. Immune mechanisms and tumor dormancy. Medicina (B Aires), *56* (Suppl. 1)*:* 74–82, 1996.
9. Yu, W., Kim, J., and Ossowski, L. Reduction in surface urokinase receptor forces malignant cells in a protracted state of dormancy. J. Cell Biol., *137:* 767–777, 1997.
10. Holmgren, L., O'Reilly, M. S., and Folkman, J. Dormancy of micrometastases: balanced proliferation and apoptosis in the presence of angiogenesis suppression. Nat. Med., *1:* 149–153, 1995.
11. Murray, C. Tumor dormancy: not so sleepy after all. Nat. Med., *1:* 117–118, 1995.
12. Uhr, J. W., Scheuermann, R. H., Street, N. E., and Vitetta, E. S. Cancer dormancy: opportunities for new therapeutic approaches. Nat. Med., *3:* 505–509, 1997.
13. Folkman, J. Angiogenesis in cancer, vascular, rheumatoid, and other disease. Nat. Med., *1:* 27–31, 1995.
14. Luzzi, K. J., MacDonald, I. C., Schmidt, E. E., Kerkvliet, N., Morris, V. L., Chambers, A. F., and Groom, A. C. Multistep nature of metastatic inefficiency: dormancy of solitary cells after successful extravasation and limited survival of early micrometastases. Am. J. Pathol., *153:* 865–873, 1998.
15. Cameron, D. M., Schmidt, E. E., Kerkvliet, N., Nadkarni, K. V., Morris, V. L., Groom, A. C., Chambers, A. F., and MacDonald, I. C. Temporal progression of metastasis in lung: cell survival, dormancy, and location dependence of metastatic inefficiency. Cancer Res., *60:* 2541–2546, 2000.
16. Morris, V. L., Koop, S., MacDonald, I. C., Schmidt, E. E., Grattan, M., Percy, D., Chambers, A. F., and Groom, A. C. Mammary carcinoma cell lines of high and low metastatic potential differ not in extravasation but in subsequent migration and growth. Clin. Exp. Metastasis, *12:* 357–367, 1994.
17. Morris, V. L., Tuck, A. B., Wilson, S. M., Percy, D., and Chambers, A. F. Tumor progression and metastasis in murine D2 hyperplastic alveolar nodule mammary tumor cell lines. Clin. Exp. Metastasis, *11:* 103–112, 1993.
18. Morris, V. L., MacDonald, I. C., Koop, S., Schmidt, E. E., Chambers, A. F., and Groom, A. C. Early interactions of cancer cells with the microvasculature in mouse liver and muscle during hematogenous metastasis: videomicroscopic analysis. Clin. Exp. Metastasis, *11:* 377–390, 1993.
19. Weiss, L., Nannmark, U., Johansson, B. R., and Bagge, U. Lethal deformation of cancer cells in the microcirculation: a potential rate regulator of hematogenous metastasis. Int. J. Cancer, *50:* 103–107, 1992.
20. Chambers, A. F., MacDonald, I. C., Schmidt, E. E., Morris, V. L., and Groom, A. C. Clinical targets for antimetastasis therapy. Adv. Cancer Res., *79:* 91–121, 2000.
21. Talmadge, J. E., Wolman, S. R., and Fidler, I. J. Evidence for the clonal origin of spontaneous metastases. Science (Wash. DC), *217:* 361–363, 1982.
22. Chambers, A. F., and Wilson, S. Use of NeoR B16F1 murine melanoma cells to assess clonality of experimental metastases in the immune-deficient chick embryo. Clin. Exp. Metastasis, *6:* 171–182, 1988.
23. Talmadge, J. E., and Zbar, B. Clonality of pulmonary metastases from the bladder 6 subline of the B16 melanoma studied by southern hybridization. J. Natl. Cancer Inst. (Bethesda), *78:* 315–320, 1987.
24. Weibel, E. R. Profile size and particle size. *In:* E. R. Weibel (ed.), Stereological Methods: Practical Methods for Biological Morphometry, Vol. 1, pp. 51–60. New York: Academic Press, Inc., 1979.
25. Chambers, A. F., Shafir, R., and Ling, V. A. Model system for studying metastasis using the embryonic chick. Cancer Res., *42:* 4018–4025, 1982.
26. Karrison, T. G., Ferguson, D. J., and Meier, P. Dormancy of mammary carcinoma after mastectomy. J. Natl. Cancer Inst. (Bethesda), *91:* 80–85, 1999.
27. Demicheli, R., Terenziani, M., Valagussa, P., Moliterni, A., Zambetti, M., and Bonadonna, G. Local recurrences following mastectomy: support for the concept of tumor dormancy. J. Natl. Cancer Inst. (Bethesda), *86:* 45–48, 1994.
28. Meltzer, A. Dormancy and breast cancer. J. Surg. Oncol., *43:* 181–188, 1990.
29. Laird, A. K. Dynamics of growth in tumors and normal organisms. J. Natl. Cancer Inst. Monogr., *30:* 15–28, 1969.
30. Speer, J. F., Petrosky, V. E., Retsky, M. W., and Wardwell, R. H. A stochastic numerical model of breast cancer growth that simulates clinical data. Cancer Res., *44:* 4124–4130, 1984.
31. Demicheli, R., Retsky, M. W., Swartzendruber, D. E., and Bonadonna, G. Proposal for a new model of breast cancer metastatic development. Ann. Oncol., *8:* 1075–1080, 1997.
32. Retsky, M. W., Demicheli, R., Swartzendruber, D. E., Bame, P. D., Wardwell, R. H., Bonadonna, G., Speer, J. F., and Valagussa, P. Computer simulation of a breast cancer metastasis model. Breast Cancer Res. Treat., *45:* 193–202, 1997.
33. Hahnfeldt, P., Panigraphy, D., Folkman, J., and Hlatky, L. Tumor development under angiogenic signaling: a dynamic theory of tumor growth, treatment response, and postvascular dormancy. Cancer Res., *59:* 4770–4775, 1999.
34. Wong, C. W., Lee, A., Shientag, L., Yu, J., Dong, Y., Kao, G., Al-Mehdi, A. B., Bernhard, E. J., and Muschel, R. J. Apoptosis: an early event in metastatic inefficiency. Cancer Res., *61:* 333–338, 2001.
35. Chekmareva, M. A., Kadkhodaian, M. M., Hollowell, C. M. P., Kim, H., Yoshida, B. A., Luu, H. H., Stadler, W. M., and Rinker-Schaeffer, C. W. Chromosome 17-mediated dormancy of AT6.1 prostate cancer micrometastases. Cancer Res., *58:* 4963–4969, 1998.
36. Goldberg, S. F., Harms, J. F., Quon, K., and Welch, D. R. Metastasis-suppressed C8161 melanoma cells arrest in lung but fail to proliferate. Clin. Exp. Metastasis, *17:* 601–607, 1999.